Gallium Energy Bands and Fermi Surface via the Augmented-Plane-Wave Method*

JOHN H. WOOD
Department of Physics, Massachusetts Institute of Technology, Cambridge, Massachusetts
(Received 13 September 1965)

Results of numerical calculations of the band structure of gallium are reported; the calculations have been carried out according to the augmented-plane-wave (APW) method of Slater. Calculations have been carried out at 115 points in $\frac{1}{8}$ of the Brillouin zone. An approximate Fermi energy is determined by counting states; cuts of surfaces of constant energy have been constructed for two energies near this approximate Fermi energy. One set of cuts is presented in this paper. The potential used was an *ad hoc* one constructed from superposed free atoms and a $\rho^{1/3}$ exchange potential; the free-atom calculations used were those of Freeman and Watson. The lattice constants are taken as supplied by Barrett, viz., $a=4.5151\times10^{-8}$ cm, $b=4.4881\times10^{-8}$ cm, and $c=7.6318\times10^{-8}$ cm. The bands resemble perturbed free-electron bands, but the two Fermi surfaces exhibit considerable departures from the free-electron Fermi surface. Because of the inherent defects in the *ad hoc* potential, it is unlikely that the present calculations can be expected to explain all the experimental information, but it is hoped that they will furnish a better zeroth-order model than does the free-electron picture.

INTRODUCTION

THE primary reason for undertaking this calculation on gallium was that gallium is a metal very well suited for experimental Fermi-surface investigations. This is due to the long mean free path (about 1 cm at 4.2°K) of the electrons which in turn leads to high resolution in the experiments.[1] It also seemed clear that the free-electron model of gallium[2,3] was not adequate to account for the experimental information then at hand.[2–7] The experiments, the free-electron model, and the augmented-plane-wave (APW) model all indicate a complicated Fermi-surface structure; it was (and is) our hope that the APW model will be of use in elucidating the details of this structure.

The particular choice of the APW method for handling the problem was made largely on the basis of expedience. There already existed computer programs for cubic structures which contained much of the necessary machinery for carrying out an energy-band calculation for any crystal structure. The changes necessary were inclusion of the fact that the real-space unit cell of gallium contains four atoms and that gallium has orthorhombic symmetry.[2] Because of the structure of the APW method this is a relatively easy task. The description of the method is given by Slater[8] and a brief description of the mechanization is given in an earlier paper by the author.[9] Because gallium possesses a center of inversion, it turns out that all machine calculations carried out at points inside the first Brillouin zone could be cast into terms of real (as distinct from complex) arithmetic, taking complete advantage of symmetry. This does not prove to be the case for some points on the surface of the zone and there the calculations were carried out using reducible representations of the group of the wave vector—this amounts to not taking full advantage of the symmetry of these points.

The calculation was a "one-shot" one—the bands derived from the assumed one-electron potential were taken as the final set. We mention this because recent work of Herman[10] Switendick,[11] and DeCicco[12] has shown how one may carry out an iterative self-consistent energy-band calculation just as is done in the case of isolated atoms. Fortunately, these calculations indicate that a superposed free atom potential is not a bad first guess at the self-consistent potential.

RESULTS OF COMPUTATIONS

The calculations reported here were performed using a one-electron muffin-tin potential. The Coulomb portion of this potential was obtained from the free-atom gallium wave functions of Watson and Freeman[13]; onto this is added a Slater $\rho^{1/3}$ exchange potential. The method of superposition of the free-atom information used is that described by Mattheiss.[14] The lattice constants used were those of Barrett[15]—$a=4.5151\times10^{-8}$ cm, $b=4.4881\times10^{-8}$ cm, and $c=7.6318\times10^{-8}$ cm. The radius of the APW sphere was 2.2989 atomic units. Two criticisms are in place here. First, those regions of the Wigner-Seitz cell lying outside the four APW spheres

* Assisted by the Office of Naval Research, the U. S. Army, Navy, and Air Force and the National Science Foundation.
[1] L. R. Weisberg and R. M. Josephs, Phys. Rev. **124**, 36 (1961). Also M. Yaqub and J. F. Cochran, Phys. Rev. Letters **10**, 390 (1963); J. F. Cochran and M. Yaqub, Phys. Letters **5**, 307 (1963).
[2] W. A. Reed and J. A. Marcus, Phys. Rev. **126**, 1298 (1962).
[3] J. C. Slater, G. F. Koster, and J. H. Wood, Phys. Rev. **126**, 1307 (1962).
[4] D. Shoenberg, Phil. Trans. Roy. Soc. London **A245**, 1 (1952).
[5] H. E. Alekseevski and Yu. P. Gaidukov, Zh. Eksperim. i Teor. Fiz. **9**, 311 (1954).
[6] J. Yahia and J. A. Marcus, Phys. Rev. **113**, 137 (1959).
[7] B. W. Roberts, Phys. Rev. Letters **6**, 453 (1961).
[8] J. C. Slater, Phys. Rev. **51**, 846 (1937).
[9] J. H. Wood, Phys. Rev. **126**, 517 (1962).
[10] F. Herman (private communication).
[11] A. C. Switendick, J. Appl. Phys. **37**, 1022 (1966).
[12] P. DeCicco, MIT, Solid State and Molecular Theory Group Quarterly Progress Reports Nos. 53, 54, and 56, (unpublished).
[13] R. E. Watson and A. J. Freeman, Phys. Rev. **124**, 1117 (1961).
[14] L. F. Mattheiss, Phys. Rev. **133**, A1399 (1964).
[15] C. S. Barrett, in *Advances in X-ray Analysis*, edited by W. M. Mueller (Plenum Press, Inc., New York, 1962), Vol. 5.

account for roughly 60% of the total cell volume; thus, in well over half the volume of the cell the potential is taken as a constant. Secondly it appears[16] that the values quoted for a and b should be, in fact, interchanged. Of these two criticisms it is likely that the first is the more quantitatively significant.

Figure 1 is a drawing of the gallium Brillouin zone. The numerical results of the calculation are listed in Tables I and II. Table I gives the energies of the lowest 4 bands which are completely filled. Table II refers to the next 4 bands, all of which are partially occupied. Figures 2 and 3 give two sample $E(\mathbf{k})$ curves as constructed from the numerical information and the compatibility relations of Ref. 3. To a first approximation these curves can be sketched simply by taking the free-electron curves of Ref. 3 and removing the accidental degeneracies present there. The free-electron $E(\mathbf{k})$ reveal a considerable number of accidental degeneracies; this may be looked at as a result of the rather low sym-

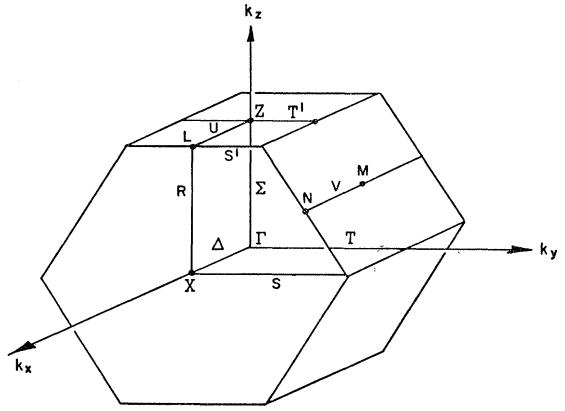

FIG. 1. Brillouin zone for gallium.

metry of the crystal. Because of the low symmetry as compared with a cubic crystal, for example, we do not have as many symbols with which to label the free electron bands and hence we might expect *a priori* more accidental degeneracies. In fact, these degeneracies occur throughout the Brillouin zone and not just at the zone boundaries. As a consequence, departure of $E(\mathbf{k})$ from free-electron behavior will occur at all these places. This explains, for example, the behavior of the bands as plotted along T and T'. In the vicinity of $E=0.4$ Ry, the Fermi energy, these bands look like anything but free-electron bands and yet this is much the same sort of picture one gets by taking the free-electron plots and removing the accidental degeneracies. It is then no surprise that the Fermi surface arising from the APW picture bears little apparent resemblance to the free-electron surface. It should be mentioned that the numerical results are all converged to about 0.01 Ry. The number of plane waves used in the expansion of the

[16] A. P. Lenham (private communication).

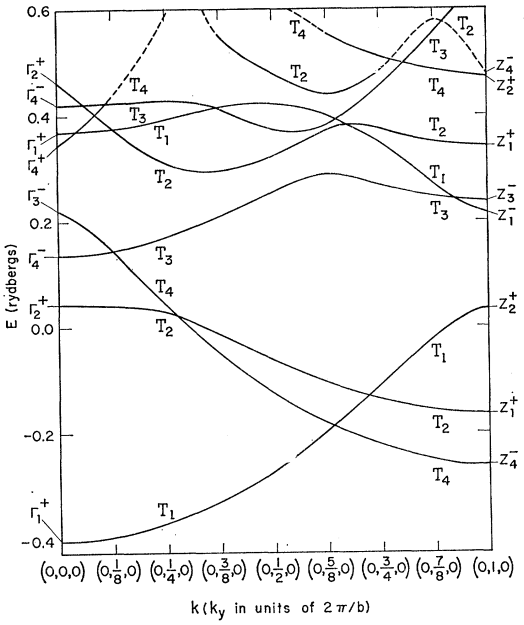

FIG. 2. Energy bands in gallium from Γ to Z along [0 1 0].

APW wave functions outside the APW spheres corresponded to using $\mathbf{k}$ vectors out to the fifth-nearest neighbors in reciprocal space. For a point of no symmetry this amounts to handling a secular equation of a size about 26×26. Improving the convergence, with the concommitance of larger secular equations, was

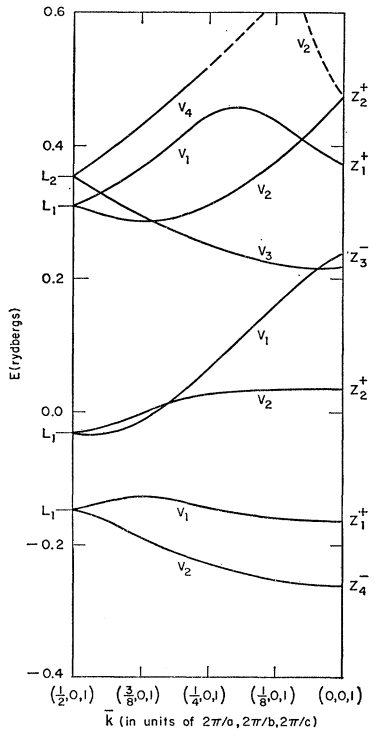

FIG. 3. Energy bands in gallium from L to Z along U.

TABLE I. Energies of 4 lowest bands. All values are in rydberg units. We give the coordinates $8\mathbf{k}$ where $\mathbf{k}$ is written in units of $2\pi/a$, $2\pi/b$, and $2\pi/c$. The symbols preceding the coordinates are Brillouin zone labels as defined in Fig. 1. Symbols preceding the energies are irreducible representation labels as defined in Ref. 3.

	8k	Band 1		Band 2		Band 3		Band 4	
Γ	0,0,0	1+	−0.402	2+	0.043	4−	0.136	3−	0.222
T	0,1,0	1	−0.395	2	0.041	3	0.144	4	0.145
T	0,2,0	1	−0.371	2	0.029	4	0.042	3	0.170
T	0,3,0	1	−0.330	4	−0.049	2	−0.014	3	0.208
T	0,4,0	1	−0.272	4	−0.124	2	−0.060	3	0.256
T	0,5,0	1	−0.194	4	−0.183	2	−0.103	3	0.287
Σ	0,0,2	1	−0.391	2	0.041	1	0.108	2	0.215
	0,1,2	+	−0.384	−	0.030	+	0.116	−	0.150
	0,2,2	+	−0.359	−	−0.024	−	0.097	+	0.140
	0,3,2	+	−0.318	−	−0.103	−	0.056	+	0.175
	0,4,2	+	−0.259	−	−0.173	−	0.010	+	0.214
Σ	0,0,4	1	−0.358	1	0.013	2	0.040	2	0.213
	0,1,4	+	−0.351	−	0.007	+	0.020	−	0.171
	0,2,4	+	−0.326	−	−0.069	+	0.042	−	0.158
	0,3,4	+	−0.286	−	−0.153	+	0.072	−	0.148
M	0,4,4	1	−0.227	1	−0.227	1	0.112	1	0.112
Σ	0,0,6	1	−0.305	1	−0.098	2	0.037	2	0.227
	0,1,6	+	−0.297	+	−0.089	−	−0.014	−	0.208
	0,2,6	+	−0.272	−	−0.100	+	−0.070	−	0.220
	0,3,6	+	−0.229	−	−0.184	+	−0.034	−	0.234
Z	0,0,8	4−	−0.261	1+	−0.164	2+	0.034	1−	0.214
T'	0,1,8	4	−0.252	2	−0.157	1	−0.020	3	0.245
T'	0,2,8	4	−0.225	2	−0.137	1	−0.110	3	0.265
Δ	1,0,0	1	−0.394	2	−0.022	2	0.197	1	0.227
	1,1,0	+	−0.388	−	−0.018	+	0.151	−	0.193
	1,2,0	+	−0.363	−	−0.011	+	0.049	−	0.177
	1,3,0	+	−0.322	+	−0.042	−	−0.025	−	0.165
	1,4,0	+	−0.262	+	−0.116	−	−0.060	−	0.186
	1,5,0	+	−0.187	+	−0.175	−	−0.099	−	0.212
	1,0,2	+	−0.383	+	−0.018	+	0.145	+	0.213
	1,1,2		−0.376		−0.017		0.117		0.176
	1,2,2		−0.352		−0.033		0.056		0.168
	1,3,2		−0.310		−0.097		0.037		0.162
	1,4,2		−0.251		−0.167		0.008		0.171
	1,0,4	+	−0.350	+	−0.017	+	0.047	+	0.170
	1,1,4		−0.344		−0.020		0.035		0.132
	1,2,4		−0.319		−0.069		0.034		0.122
	1,3,4		−0.277		−0.147		0.062		0.122
V	1,4,4	1	−0.220	2	−0.220	1	0.099	2	0.099
	1,0,6	+	−0.297	+	−0.093	+	0.029	+	0.159
	1,1,6		−0.288		−0.084		−0.011		0.146
	1,2,6		−0.264		−0.090		−0.064		0.155
	1,3,6		−0.220		−0.179		−0.032		0.175
U	1,0,8	2	−0.253	1	−0.158	2	0.034	1	0.160
	1,1,8	−	−0.242	+	−0.150	−	−0.016	+	0.168
	1,2,8	−	−0.217	+	−0.132	−	−0.103	+	0.189
Δ	2,0,0	1	−0.370	2	−0.113	1	0.246	2	0.270
	2,1,0	+	−0.363	−	−0.107	+	0.173	−	0.249
	2,2,0	+	−0.339	−	−0.091	+	0.072	−	0.192
	2,3,0	+	−0.296	−	−0.071	+	−0.018	−	0.134
	2,4,0	+	−0.240	+	−0.093	−	−0.070	−	0.110
	2,5,0	+	−0.172	+	−0.150	−	−0.093	−	0.106
	2,0,2	+	−0.359	+	−0.105	+	0.190	+	0.222
	2,1,2		−0.352		−0.099		0.135		0.204
	2,2,2		−0.327		−0.087		0.047		0.185
	2,3,2		−0.287		−0.096		−0.007		0.139
	2,4,2		−0.230		−0.147		−0.009		0.099
	2,0,4	+	−0.325	+	−0.084	+	0.071	+	0.156
	2,1,4		−0.317		−0.079		0.061		0.112
	2,2,4		−0.293		−0.080		0.014		0.100
	2,3,4		−0.254		−0.133		0.014		0.088
V	2,4,4	1	−0.198	2	−0.198	1	0.052	2	0.052
	2,0,6	+	−0.274	+	−0.089	+	0.001	+	0.100
	2,1,6		−0.264		−0.083		−0.012		0.076
	2,2,6		−0.242		−0.088		−0.048		0.071
	2,3,6		−0.202		−0.159		−0.028		0.087
U	2,0,8	2	−0.226	1	−0.142	2	0.027	1	0.061
	2,1,8	−	−0.217	+	−0.136	−	−0.009	+	0.068
	2,2,8	−	−0.197	+	−0.120	−	−0.088	+	0.087
Δ	3,0,0	1	−0.329	2	−0.196	1	0.276	2	0.313
	3,1,0	+	−0.321	−	−0.189	+	0.208	−	0.274
	3,2,0	+	−0.297	−	−0.172	+	0.108	−	0.194
	3,3,0	+	−0.258	−	−0.141	+	0.019	−	0.113
	3,4,0	+	−0.204	−	−0.105	+	−0.054	−	0.054
	3,5,0	+	−0.145	+	−0.109	−	−0.089	−	0.019
	3,0,2	+	−0.318	+	−0.186	+	0.218	+	0.237
	3,1,2		−0.309		−0.180		0.166		0.218
	3,2,2		−0.286		−0.162		0.075		0.167
	3,3,2		−0.246		−0.135		−0.004		0.096
	3,4,2		−0.194		−0.128		−0.040		0.032
	3,0,4	+	−0.283	+	−0.159	+	0.096	+	0.150
	3,1,4		−0.276		−0.154		0.090		0.116
	3,2,4		−0.255		−0.138		0.026		0.090
	3,3,4		−0.215		−0.129		−0.025		0.041
V	3,4,4	1	−0.167	2	−0.167	1	−0.011	2	−0.011
	3,0,6	+	−0.233	+	−0.124	+	−0.003	+	0.066
	3,1,6		−0.224		−0.116		−0.003		0.049
	3,2,6		−0.204		−0.107		−0.025		0.023
	3,3,6		−0.160		−0.134		−0.038		0.009
U	3,0,8	2	−0.190	1	−0.127	1	−0.014	2	−0.003
	3,1,8	−	−0.181	+	−0.120	−	−0.015	+	−0.008
	3,2,8	−	−0.157	+	−0.106	−	−0.064	+	0.005
X	4,0,0	1	−0.274	1	−0.274	1	0.305	1	0.305
S	4,1,0	1	−0.263	1	−0.263	1	0.248	1	0.248
S	4,2,0	1	−0.240	1	−0.240	1	0.159	1	0.159
S	4,3,0	1	−0.203	1	−0.203	1	0.072	1	0.072
S	4,4,0	1	−0.155	1	−0.155	1	−0.002	1	−0.002
S	4,5,0	1	−0.109	1	−0.109	1	−0.053	1	−0.053
R	4,0,2	1	−0.260	2	−0.260	1	0.238	2	0.238
	4,1,2		−0.251		−0.251		0.200		0.200
	4,2,2		−0.231		−0.231		0.119		0.119
	4,3,2		−0.195		−0.195		0.039		0.039
	4,4,2		−0.151		−0.151		−0.026		−0.026
R	4,0,4	1	−0.229	2	−0.229	1	0.128	2	0.128
	4,1,4		−0.221		−0.221		0.115		0.115
	4,2,4		−0.201		−0.201		0.061		0.061
	4,3,4		−0.169		−0.169		−0.005		−0.005
N	4,4,4	1	−0.144	2	−0.144	3	−0.047	4	−0.047
R	4,0,6	1	−0.181	2	−0.181	1	0.028	2	0.028
	4,1,6		−0.174		−0.174		0.025		0.025
	4,2,6		−0.153		−0.153		0.002		0.002
	4,3,6		−0.130		−0.130		−0.039		−0.039
L	4,0,8	1	−0.145	1	−0.145	1	−0.029	1	−0.029
S'	4,1,8	1	−0.138	1	−0.138	1	−0.030	1	−0.030
S'	4,2,8	1	−0.116	1	−0.116	1	−0.045	1	−0.045

judged too expensive. A number of tests indicate that the qualitative features of the bands are not changed when convergence is improved—it is doubtful that the quantitative improvement would be significant in any event.

The number of electrons to be accommodated in these bands is 12 per cell—we have four atoms per cell and three electrons $4s^24p$ from each atom. Each band can accommodate 2 electrons per cell and so we must have, on the average, six full bands. The Fermi energy was determined by counting of states and was thus determined to be at $E_F=+0.405$ Ry on an (arbitrary) energy scale where the energy of the lowest Γ_1^+ is at -0.402 Ry. The width of the occupied bands is thus 0.807 Ry as contrasted with the corresponding free-electron value of 0.774 Ry. This particular method of

TABLE II. Energies of bands, 5, 6, 7, and 8; these bands are partially occupied up to E_F. Units and nomenclature are those of Table I. Energies have been listed up to 0.500 Ry on our (arbitrary) energy scale.

8k	Band 5	Band 6	Band 7	Band 8
Γ 0,0,0	4+ 0.345	1+ 0.368	4− 0.421	2+ 0.463
T 0,1,0	2 0.374	1 0.375	3 0.424	4 0.436
T 0,2,0	2 0.310	1 0.393	3 0.427	
T 0,3,0	2 0.293	3 0.412	1 0.416	
T 0,4,0	2 0.321	3 0.373	1 0.420	2 0.481
T 0,5,0	2 0.372	3 0.381	1 0.400	2 0.441
Σ 0,0,2	1 0.277	4 0.310	2 0.494	
0,1,2	+ 0.284	− 0.391	− 0.420	
0,2,2	+ 0.304	− 0.335		
0,3,2	− 0.309	+ 0.329		
0,4,2	− 0.331	+ 0.345	− 0.453	
Σ 0,0,4	4 0.262	1 0.266		
0,1,4	+ 0.274	− 0.350	− 0.481	
0,2,4	+ 0.298	− 0.398	− 0.474	
0,3,4	+ 0.330	− 0.351	+ 0.448	− 0.486
M 0,4,4	1 0.345	1 0.345	1 0.432	1 0.432
Σ 0,0,6	4 0.230	1 0.307		
0,1,6	− 0.306	+ 0.315		
0,2,6	+ 0.339	− 0.398	− 0.450	+ 0.490
0,3,6	+ 0.363	− 0.377	+ 0.427	− 0.457
Z 0,0,8	3− 0.238	1+ 0.342	2+ 0.472	4− 0.478
T′ 0,1,8	1 0.268	2 0.350	4 0.487	
T′ 0,2,8	1 0.349	2 0.373	3 0.457	2 0.481
Δ 1,0,0	4 0.353	1 0.374	2 0.417	3 0.493
1,1,0	+ 0.380	− 0.381	− 0.441	+ 0.443
1,2,0	− 0.344	+ 0.394	− 0.420	
1,3,0	− 0.341	− 0.383	+ 0.405	
1,4,0	− 0.297	+ 0.388	− 0.411	
1,5,0	− 0.286	+ 0.352	− 0.460	
1,0,2	+ 0.315	− 0.318		
1,1,2	0.309	0.399	0.437	
1,2,2	0.291	0.387	0.481	
1,3,2	0.281	0.370	0.451	
1,4,2	0.270	0.368	0.461	
1,0,4	− 0.268	+ 0.345		
1,1,4	0.328	0.363	0.466	
1,2,4	0.330	0.386	0.458	0.486
1,3,4	0.296	0.339	0.474	
V 1,4,4	1 0.296	2 0.296		
1,0,6	− 0.236	+ 0.392	+ 0.427	
1,1,6	0.294	0.399	0.450	0.467
1,2,6	0.356	0.364	0.416	
1,3,6	0.289	0.389	0.431	
U 1,0,8	3 0.223	2 0.376	1 0.436	
1,1,8	− 0.262	− 0.412	+ 0.442	+ 0.460
1,2,8	− 0.310	+ 0.356	+ 0.461	
Δ 2,0,0	4 0.377	1 0.391	2 0.418	
2,1,0	− 0.391	+ 0.394	+ 0.462	− 0.468
2,2,0	− 0.347	+ 0.393	− 0.433	
2,3,0	− 0.281	+ 0.365	− 0.456	
2,4,0	− 0.220	+ 0.315		
2,5,0	− 0.199	+ 0.267		
2,0,2	− 0.344	+ 0.385		
2,1,2	0.351	0.415	0.459	
2,2,2	0.300	0.383	0.500	
2,3,2	0.259	0.350	0.454	
2,4,2	0.213	0.360	0.419	
2,0,4	− 0.296	+ 0.426	+ 0.454	
2,1,4	0.340	0.388	0.460	0.465
2,2,4	0.300	0.376	0.424	
2,3,4	0.256	0.329	0.449	
V 2,4,4	1 0.277	2 0.277		
2,0,6	− 0.261	+ 0.342	+ 0.455	
2,1,6	0.266	0.365	0.407	
2,2,6	0.267	0.289		
2,3,6	0.208	0.326	0.458	
U 2,0,8	3 0.252	2 0.310	1 0.445	
2,1,8	− 0.231	+ 0.356	− 0.390	
2,2,8	− 0.235	+ 0.257		
Δ 3,0,0	1 0.413	4 0.415	2 0.422	3 0.500
3,1,0	− 0.388	+ 0.406	− 0.477	+ 0.489
3,2,0	− 0.311	+ 0.368	− 0.488	
3,3,0	− 0.235	+ 0.303		
3,4,0	− 0.177	+ 0.243		
3,5,0	− 0.150	+ 0.195		
3,0,2	− 0.384	+ 0.440	+ 0.473	− 0.496
3,1,2	0.375	0.404	0.453	
3,2,2	0.330	0.360	0.455	0.470
3,3,2	0.264	0.348	0.411	
3,4,2	0.205	0.298	0.441	
3,0,4	− 0.337	+ 0.377	+ 0.412	− 0.462
3,1,4	0.310	0.326	0.464	
3,2,4	0.258	0.323	0.449	
3,3,4	0.259	0.339	0.392	0.490
V 3,4,4	1 0.295	2 0.295	1 0.423	2 0.423
3,0,6	− 0.304	+ 0.308	+ 0.378	− 0.436
3,1,6	0.235	0.288	0.427	
3,2,6	0.203	0.223		
3,3,6	0.178	0.250		
U 3,0,8	2 0.285	3 0.293	1 0.365	4 0.426
3,1,8	− 0.206	+ 0.275	− 0.414	
3,2,8	− 0.178	+ 0.187		
X 4,0,0	1 0.421	1 0.421	2 0.461	2 0.461
S 4,1,0	1 0.395	1 0.395		
S 4,2,0	1 0.328	1 0.328		
S 4,3,0	1 0.255	1 0.255		
S 4,4,0	1 0.190	1 0.190		
S 4,5,0	1 0.152	1 0.152		
R 4,0,2	3 0.438	4 0.438	1 0.443	2 0.443
4,1,2	0.385	0.385	0.484	0.484
4,2,2	0.363	0.363	0.427	0.427
4,3,2	0.301	0.301	0.444	0.444
4,4,2	0.238	0.238	0.493	0.493
R 4,0,4	1 0.370	2 0.370	3 0.392	4 0.392
4,1,4	0.294	0.294		
4,2,4	0.273	0.273		
4,3,4	0.295	0.295	0.424	0.424
N 4,4,4	1 0.328	2 0.328	3 0.367	4 0.367
R 4,0,6	1 0.325	2 0.325	3 0.362	4 0.362
4,1,6	0.238	0.238	0.477	0.477
4,2,6	0.189	0.189		
4,3,6	0.197	0.197		
L 4,0,8	1 0.309	1 0.309	2 0.352	2 0.352
S′ 4,1,8	1 0.221	1 0.221	1 0.466	1 0.466
S′ 4,2,8	1 0.159	1 0.159		

Fermi-level determination is not nearly so elegant as that of Loucks[17] but we felt that the coarse grain of our information did not justify use of his method. Once the Fermi energy has been determined it is a straightforward task to determine the Fermi surface. This was done by graphical methods—the $E(\mathbf{k})$ were plotted in many directions and the $\mathbf{k}$ points at which these bands cut through E_F were determined. This collection of points was then plotted and connected together by hand. This procedure was carried out for two different choices of E_F, viz., $E_F=0.400$ Ry and $E_F=0.410$ Ry, which bracket the aforementioned 0.405 Ry. Our current inclination is that the $E_F=0.400$ Ry set is more closely in agreement with available experimental information than is the latter set. However, the questions are far from being all answered and the author will be

[17] T. L. Loucks, Phys. Rev. 134, A1618 (1964).

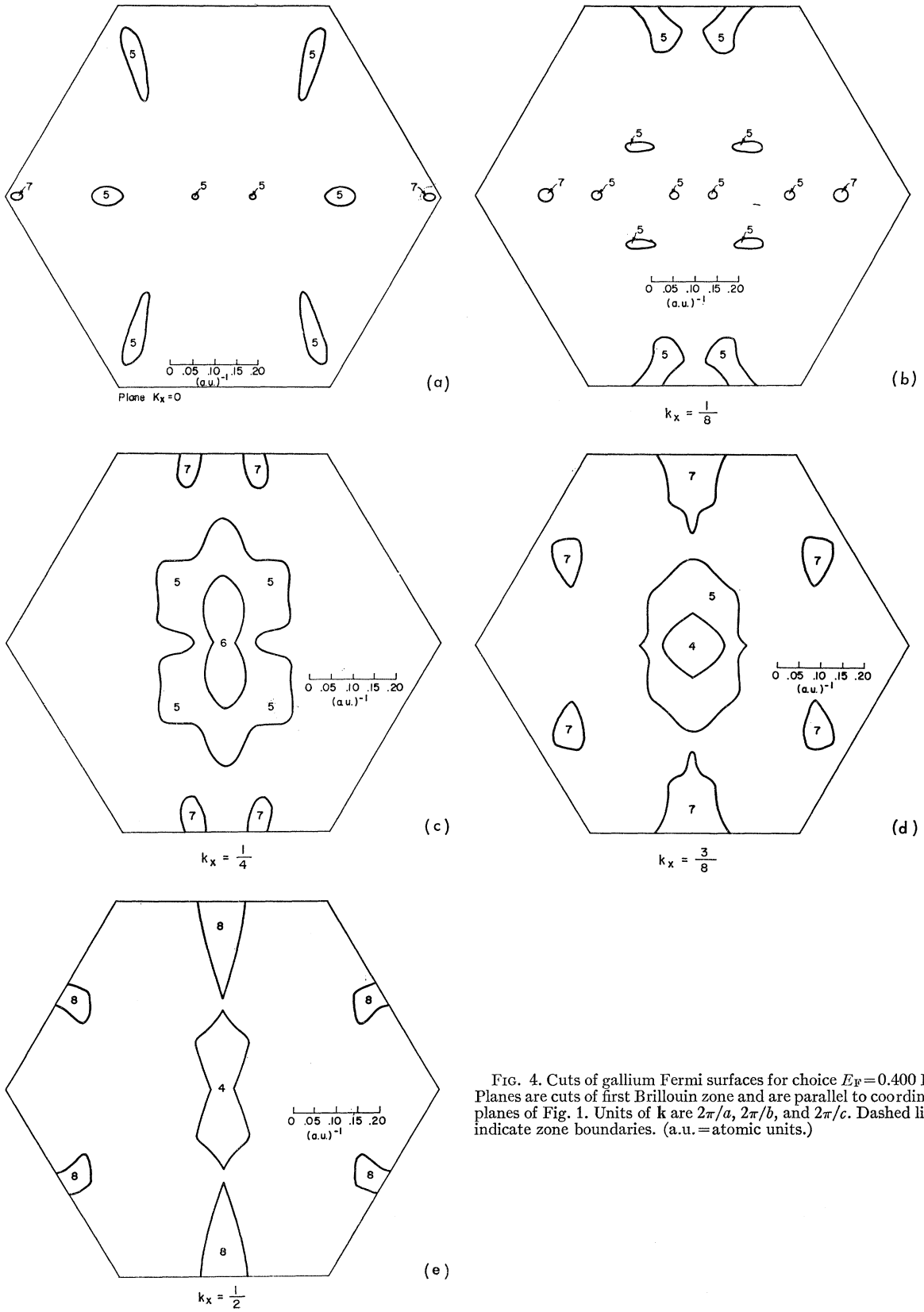

FIG. 4. Cuts of gallium Fermi surfaces for choice $E_F = 0.400$ Ry. Planes are cuts of first Brillouin zone and are parallel to coordinate planes of Fig. 1. Units of **k** are $2\pi/a$, $2\pi/b$, and $2\pi/c$. Dashed lines indicate zone boundaries. (a.u. = atomic units.)

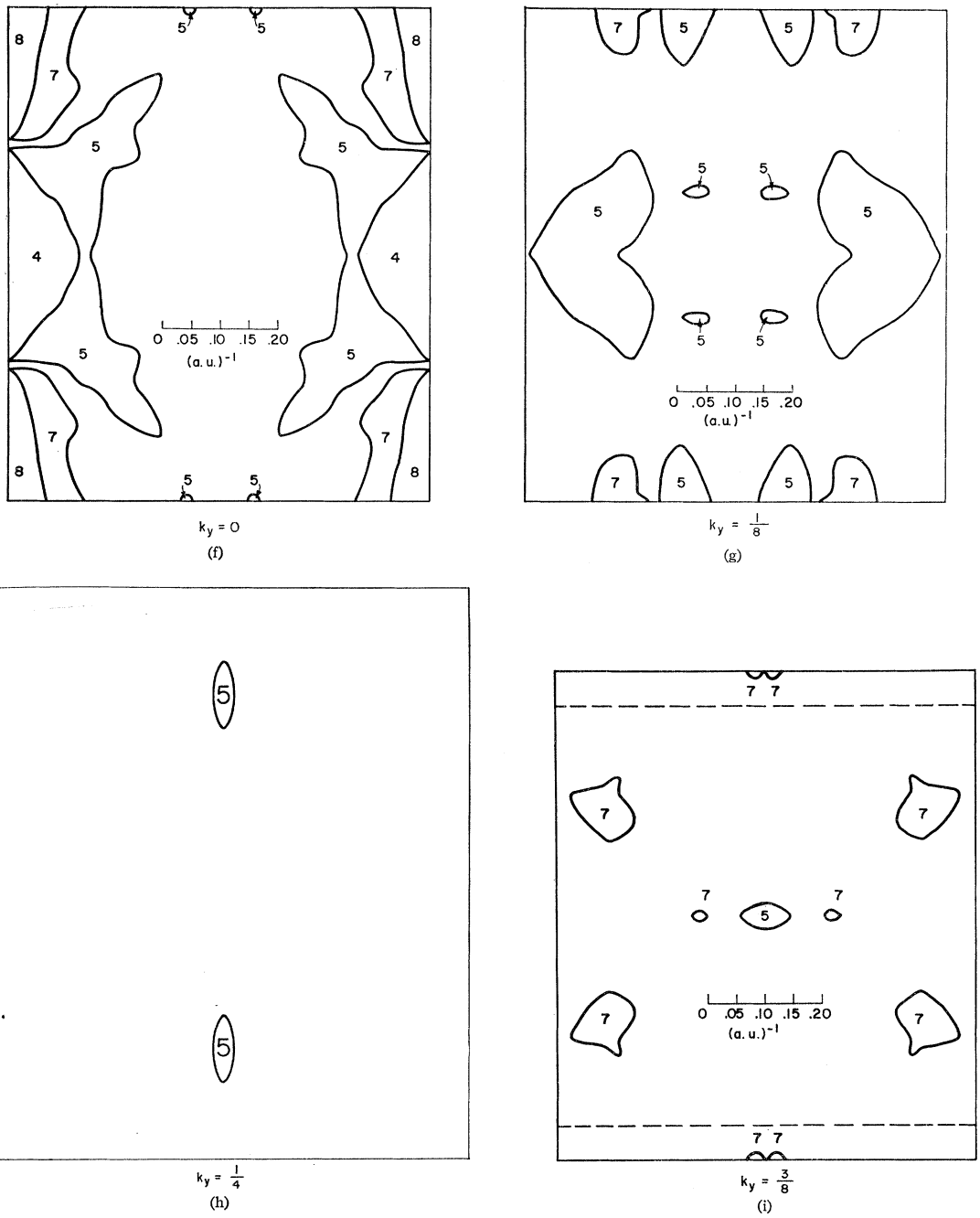

(*Figure 4 continued on next page.*)

happy to supply copies of the $E_F=0.410$ set, which is not presented here.

We have not included perspective drawings of the surfaces but only the cuts through certain planes. Perspective drawings appear in the paper of Goldstein and Foner.[18] We have chosen three sets of planes; each set is parallel to one of the three coordinate planes of **k** space. For example, the hexagons are planes parallel to the k_yk_z (or bc) plane. The notation under each hexagon indicates the k_x coordinate of the hexagon. The dashed lines in the figures indicate the boundaries of the first Brillouin zone; the center of each figure is always in the first zone and those cuts which lie on the other side of the dashed lines are in the neighboring zone. [It should be mentioned that there is an additional symmetry present in gallium which is not dis-

[18] A. Goldstein, Ph.D. thesis, Department of Physics, Massachusetts Institute of Technology, 1965 (unpublished); A. Goldstein and S. Foner, following paper, Phys. Rev. **146**, 442 (1966).

FIG. 4 (*continued*).

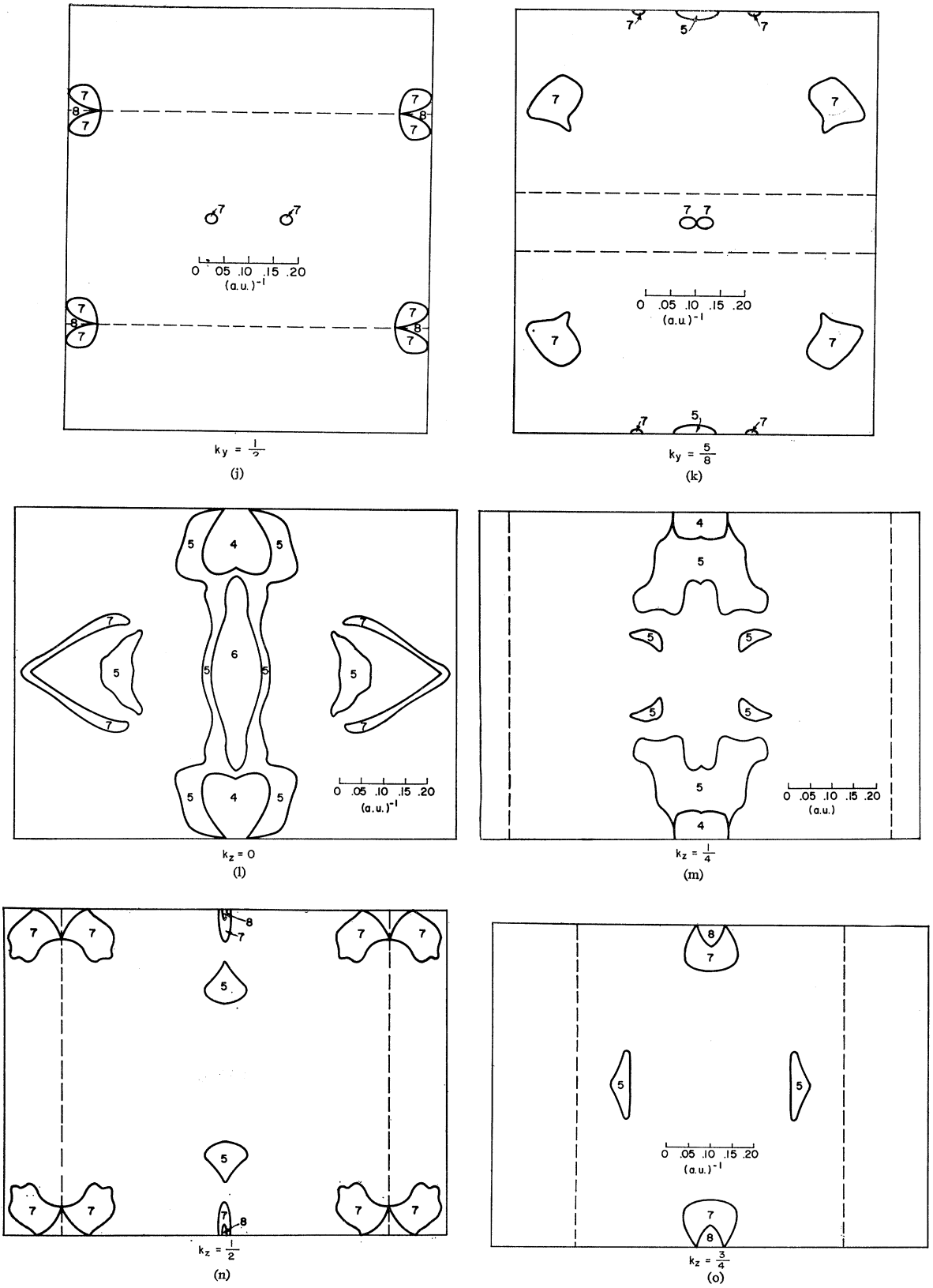

FIG. 4 (*continued*).

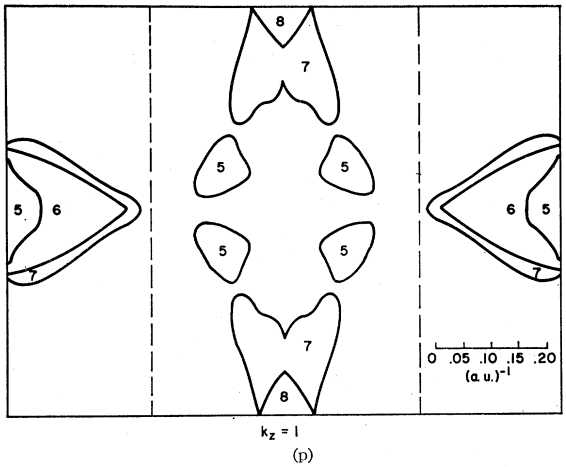

played by the zone itself. Consider a point lying on the boundary plane which contains points N and M, and the line V. If this point is reflected in the line V then the energies associated with the reflected point (which lies in this same plane) are identical with those at the original point. This is true only for points precisely on the plane; this situation is analogous to the equivalence of the K and U of the fcc reciprocal lattice where again the points are not carried into one another by an operation of the point group but by an operation of the space group.]

Let us now comment on the Fermi surface taking the set for $E_F=0.400$ first. Each cut was drawn as indicated previously but the number of points was rarely in excess of 24 for any given contour—thus the detailed shape of a contour must not be taken too seriously. In addition, because of the discreteness of the grid of **k** points, it is entirely possible that some small pieces of the surface have been completely missed. One point seems quite clear. Neither this set nor the set corresponding to $E_F=0.410$ Ry yields open orbits along the k_z or c direction—this was a clear-cut conclusion of Reed and Marcus.

Let us now consider the main pieces predicted by the present calculations. First, we have what we may call band-8 electron surfaces. The center of one of these surfaces is at the point L; in the $k_z=1$ cut the intersection of this surface appears "behind the butterfly." The surface cuts into three neighboring zones and is essentially a flattened cigar with the major axis in the c direction. The other band-8 surface is the smaller piece centered about N (see $k_x=\frac{1}{2}$ cut) which again extends into three neighboring zones. This piece is severely pinched in the a direction (see $k_y=\frac{1}{2}$ cut). Next consider the band-7 electron surfaces. The largest of these consists of the surface which intersects the $k_z=1$ plane in the butterfly although, of course, the back end of the butterfly is not a part of this surface. This surface extends into the same three neighboring zones as does the flattened cigar. Because of the extra (time-reversal induced) degeneracy on the hexagonal face the extent of this surface in the c direction is the same as that of the cigar—we might call this a cigar with a double pair of wings. Another one of these surfaces is the wishbone-shaped object which lies in the $k_z=0$ plane. As can be seen from the plots perpendicular to the k_y or b axis, the legs of the wishbone are indeed small in cross section and this surface is closely localized to $k_z=0$. A third of these surfaces is one centered on N which surrounds the second band-8 surface. In the $k_z=\frac{1}{2}$ plane, this is the surface which looks like a distorted bell.

Next, consider the band-6 hole surfaces. These are the most complex surfaces and looking at the $k_z=0$ cut, we see that they would allow open orbits in the a direction. The major one of these surfaces has its bulk located about the $k_x=\frac{1}{2}$ plane with tubes or legs connecting through the zone to its mirror image on the $k_x=-\frac{1}{2}$ plane. Starting with the $k_x=\frac{1}{2}$ cut and moving down to the $k_x=\frac{1}{4}$ cut we see that the bulk of this object (called a two-headed six-legged camel by Goldstein and Foner[18]) increases. At about $k_x=\frac{1}{2}$, the main body of this surface terminates and connection is made to its mirror image by the tubes or legs. Two of these tubes can be seen in the $k_z=0$ cut. With the information at hand, it is not possible to decide whether there are other tubes connecting in this fashion. For example, examination of the $k_x=\frac{1}{8}$ cut shows the intersection of the aforementioned two tubes; in addition, however, there are the elliptically shaped band-6 cuts. Examination of the cuts of this particular surface in the k_y and k_z cuts suggest that these correspond to isolated surfaces but it is also possible that they correspond to tubes which are bowed in the k_y and k_z directions.[18] In addition to the camel there are the surfaces consisting of 4 "polyps" centered around the point Z. (See e.g., $k_z=1$ and $k_x=\frac{1}{8}$ cuts.) There are also the crescent-shaped surfaces lying in the $k_z=0$ planes (see $k_z=0$ and $k_x=0$ cuts); these appear to be isolated surfaces which have nothing to do with the camel. The largest elliptical shaped objects in the $k_x=0$ cut may be the intersection of the bowed legs, they may be isolated pieces, or they may represent additional portions of the polyps. The remaining surface is the band-5 hole surface which is centered about point X and extends, clearly, into the neighboring zone. This object is elongated as the k_x and k_z directions, having small extent in k_y.

As can be seen, the present calculation is suggestive rather than definitive—it is evident that a finer grained picture of k space is needed to unambiguously assign the surfaces. The second set of cuts corresponding to the choice $E_F=0.410$ Ry is similar to the first. With the increase in the assumed Fermi energy, the hole surfaces have shrunk and the electronsur faces have expanded. The general shape of many surfaces seems much the same in the two pictures. Again, however, we observe

no indication of connectivity in the k_z direction. Moreover, the two legs of the camel which lay in the $k_z=0$ plane have been pinched off, destroying the connectivity along k_x. We also obtain a new band-7 electron surface where these legs were formerly located. As mentioned earlier, we are at present inclined to regard the $E_F=0.400$ Ry set of pictures as that closest to experiment.

CORRELATION WITH FERMI SURFACE EXPERIMENTS

A fair amount of Fermi-surface data has become available recently, a good deal of which is yet unpublished. Let us first consider Figs. 4, 5, 6, and 8 of the recent work of Bezugly, Galkin, and Zhevago (BGZ).[19] Figure 4 indicates the band-8 electron surface. Compared with the free-electron situation, the experimental figure seems to have become shorter and fatter. The corresponding APW curve (see $k_x=\frac{1}{2}$ cut) for $E_F=0.400$ is also somewhat shorter but has fattened very little. The $E_F=0.410$ curve seems to be a good deal too long.

The experimental points shown in Fig. 5 of BGZ are associated with the free-electron band 7. We are inclined to associate these points with the band-6 hole surface (the camel)—cf. $k_x=\frac{1}{4}$ cut for $E_F=0.400$. The plotted points fit this portion of the surface to within about 10% if we associate the experimental points with the right-angled shoulder of the hole surface. In Fig. 6, the experimental points are associated with a band-9 electron surface. This piece is too small for us to consider. Our only comment is that it is unlikely that there are any band-9 electron surfaces present in gallium.

Considering 8 of the BGZ, the separation of the wings of the butterfly at $k_z=1$ agrees quite well with the corresponding separation of the APW butterfly. However, the location of the head of the APW butterfly is about 40% farther from the zone boundary than the experimental head. On the other hand, for the separation of the rear wing tips, we find virtually perfect agreement. Considering the cross section of the band-8 cigar which also appears in this figure we find good agreement with the k_a dimension of the cigar and (extrapolating their points) good agreement with the k_b dimension.

Some very recent work of A. Fukumoto[20] using geometric resonance with L-band ultrasonic waves has resulted in a tracing of what appears to be again associated with the camel. This unpublished curve looks a good deal like the cut of the camel through the $k_x=\frac{3}{8}$ plane provided we shrink the k_y dimension by about 25%. He observes a definite shoulder about 35 deg from the k_z axis which is very close to the location of the shoulder in the APW trace. His last data point is 20 deg from k_z so it is difficult to estimate the k_z extent of the surface. This information indicates that the broadening of the camel observed in the $k_x=\frac{1}{4}$ cut does not in fact occur.

The work of Tepley[21] which preceded that of Fukumoto also consisted of application of ultrasonic techniques. This work yielded values of extremal *linear* dimensions of Fermi surfaces. Tepley has tabulated in his thesis extremal dimensions parallel to k_x, parallel to k_y and parallel to k_z. Some, but not all, of these linear dimensions check the APW linear dimensions very well indeed. However, at the time of this work Tepley did not know which linear dimension went with which surface; this means that it is not known which extremal dimensions should be paired together and associated with a single surface. The lack of this constraint is a serious one and we feel it hardly fair to call on Tepley's results for confirmation or rejection of the APW surfaces.

Comparison with the work of Sparlin and Schreiber[22] is complicated by the fact that the dimensions indicated for the Brillouin zone appear incorrect. The two elliptical sections which they have observed may correspond to the spin-orbit split[23] band-7 and band-8 electron surfaces appearing on the $k_x=\frac{1}{2}$ cut.

The recent de Haas–van Alphen (DHVA) work of Goldstein and Foner[18] also lends some credence to the APW model. A large closed surface is found whose topology is similar to the largest sections of bands 4 and 7. By assuming that partial magnetic breakdown occurs they have made identification with band 7 and also can identify band 8 in the data. Certain pieces of DHVA data are consistent with the band-6 camel; in particular, their high-field data when extrapolated to the b axis indicates an orbit perpendicular to the k_y axis which has an area very close to that of a 4-head camel orbit—this is the orbit defined by the joining together of two camels at the hexagonal face (see $k_y=0$ cut). The details of these identifications appear in Ref. 18; the numerical agreement between the DHVA data and the APW model is not spectacular with areas disagreeing by as much as a factor of 2.

There are other experimental data on gallium[24–26] including, in particular, the early work of Shoenberg[4] and the recent work of Condon.[24] Some of this information sheds light on the smaller pieces of Fermi surface

[19] P. A. Bezugly, A. A. Galkin, and S. E. Zhevago, Zh. Eksperim. i Teor. Fiz. **47**, 825 (1964) [English transl.: Soviet Phys.—JETP **20**, 552 (1965); Fiz. Tverd. Tela **7**, 480 (1965) [English transl.: Soviet Phys. Solid State **7**, 383 (1965)].

[20] A. Fukumoto, Massachusetts Institute of Technology, Quarterly Progress Report No. 78, Research Laboratory of Electronics (unpublished).

[21] N. Tepley, Ph.D. thesis, Department of Physics, Massachusetts Institute of Technology, 1963 (unpublished); N. Tepley and M. W. P. Strandberg, Bull. Am. Phys. Soc. **9**, 58 (1964).

[22] D. M. Sparlin and D. S. Schreiber, *Proceedings of the Ninth International Conference on Low Temperature Physics, Columbus, Ohio, 1964*, edited by J. G. Daunt, D. V. Edwards, F. J. Milford, and M. Yaqub (Plenum Press, Inc., New York, 1965).

[23] G. F. Koster, Phys. Rev. **127**, 2044 (1962).

[24] J. H. Condon, Bull. Am. Phys. Soc. **1**, 239 (1964).

[25] M. Yaqub and J. F. Cochran, Phys. Rev. **137**, A1182 (1965).

[26] J. F. Cochran and C. A. Shiffman, Phys. Rev. **140**, A1678 (1965).

about which the present calculations have little to say since these small pieces are rather ill-defined in the calculations.

The limited comparison carried out here gives a reasonable idea of the number of grains of salt one should take in assessing the calculations. The major failure of the model appears to be the absence of open orbits in the c direction. The temptation is to join the band-8 cigars together along with the c direction. However, it seems that forcing this would seriously modify the topology of the band-6 camel in which we have some confidence. Another possible distortion suggested by Goldstein and Foner[18] is the joining together of the camel heads and the polyps (see $k_y=0$ cut). This seems more reasonable than the distortion of the cigars.

DENSITY OF STATES

In Fig. 5 is given a curve which indicates the filling of the bands as a function of energy. For example, the Fermi energy is the abscissa corresponding to an ordinate of 12 electrons per cell. As can be seen, this curve is quite similar to the corresponding free electron curve which is also plotted on that figure.

Figure 6 is a density-of-states curve which has been determined from the curve in Fig. 5 by a (crude) numerical-differentiation procedure. We also show the corresponding free electron curve. Again, because of the rather large size of the mesh in k space, this figure should not be taken too seriously. The electronic specific heat of gallium has been measured by a number of people,[27–29] the values of the constant γ in the expression $C_{el}=\gamma T$ range from about 0.6 to 0.75 mJ mole^{-1} deg^{-2}. The value we calculate from the figure using the density of states at the APW Fermi energy is 0.9 in these units. Thus, while the calculation indicates a reduction in the density of states at the Fermi energy this reduction is not sufficient to obtain agreement.

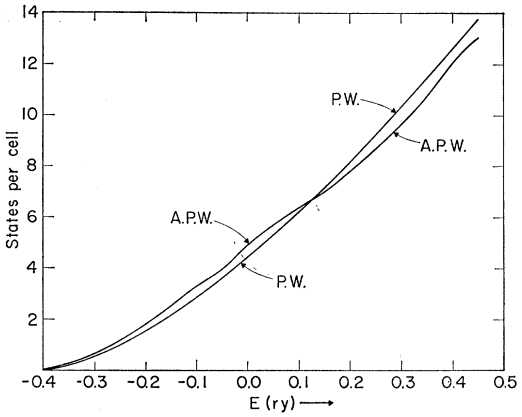

FIG. 5. Number of states per cell available at a given energy for gallium. PW shows free-electron curve, APW indicates results of this calculation.

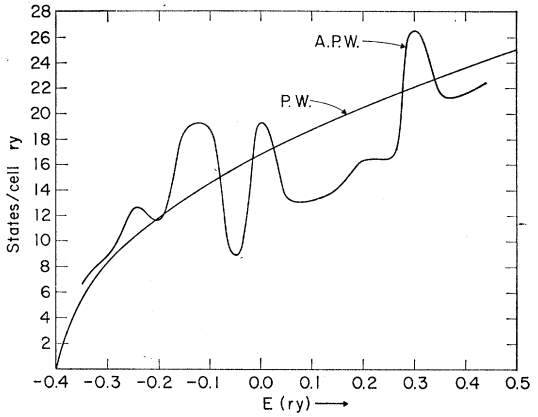

FIG. 6. Density-of-states curve for gallium. PW shows free-electron case; APW indicates results of this calculation.

SUMMARY

The APW calculation of the s and p bands of gallium has yielded a set of $E(\mathbf{k})$ which can be qualitatively described as a perturbed free-electron structure. The resulting Fermi surface bears little resemblance to the free-electron Fermi surface. It appears that the proposed surface makes some sense when compared with experiment and it is hoped that the surface will be useful as a rough guide in interpreting further experiments. We have no guarantee that our *ad hoc* muffin-tin potential is the best single potential for use in generating a band structure to be compared with experiment. Thus, it is extremely unlikely that the present calculation is the final word on the electronic structure of gallium and one should feel no trepidation in deforming the results to force agreement with experiment. In particular, it would be useful to carry out a calculation including spin-orbit effects which, as Koster[23] has shown, can be expected to qualitatively modify the Fermi surfaces. In particular, most of the time reversal degeneracy in the $k_x=\frac{1}{2}$ hexagonal face will be removed and, as Goldstein and Foner[18] point out, this could be rather important.

ACKNOWLEDGMENTS

The writer thanks Professor J. C. Slater and Professor G. F. Koster for continued support. He is indebted to A. Goldstein and S. Foner for making available the results of their work prior to publication. Thanks are due to L. F. Mattheiss and A. C. Switendick for many helpful discussions.

The computing facilities used in these calculations were those of the Lincoln Laboratory and the MIT Cooperative Computing Laboratory whose staffs have been remarkably helpful and tolerant.

[27] N. M. Wolcott, Bull. Am. Phys. Soc. **1**, 289 (1956).
[28] G. Seidel and D. H. Keesom, Phys. Rev. **112**, 1083 (1958).
[29] N. E. Phillips, Phys. Rev. **134**, A385 (1964).